

D-carbon: Ab initio study of a novel carbon allotrope

Dong Fan, Shaohua Lu, Andrey A. Golov, Artem A. Kabanov, and Xiaojun Hu

Citation: *The Journal of Chemical Physics* **149**, 114702 (2018); doi: 10.1063/1.5037380

View online: <https://doi.org/10.1063/1.5037380>

View Table of Contents: <http://aip.scitation.org/toc/jcp/149/11>

Published by the [American Institute of Physics](#)

PHYSICS TODAY

WHITEPAPERS

ADVANCED LIGHT CURE ADHESIVES

Take a closer look at what these environmentally friendly adhesive systems can do

READ NOW

PRESENTED BY
 **MASTERBOND**
ADHESIVES | SEALANTS | COATINGS

D-carbon: *Ab initio* study of a novel carbon allotrope

Dong Fan,¹ Shaohua Lu,^{1,a)} Andrey A. Golov,² Artem A. Kabanov,² and Xiaojun Hu^{1,b)}

¹College of Materials Science and Engineering, Zhejiang University of Technology, Hangzhou 310014, China

²Samara Center for Theoretical Materials Science (SCTMS), Samara University, 443011 Samara, Russia

(Received 24 April 2018; accepted 4 September 2018; published online 20 September 2018)

By means of *ab initio* computations and the global minimum structure search method, we have investigated structural, mechanical, and electronic properties of D-carbon, a crystalline orthorhombic sp^3 carbon allotrope (space group $Pmma$ [D_{2h}^5] with 6 atoms per cell). Total-energy calculations demonstrate that D-carbon is energetically more favorable than the previously proposed T_6 structure (with 6 atoms per cell) as well as many others. This novel phase is dynamically, mechanically, and thermally stable at zero pressure and more stable than graphite beyond 63.7 GPa. D-carbon is a semiconductor with a bandgap of 4.33 eV, less than diamond's gap (5.47 eV). The simulated X-ray diffraction pattern is in satisfactory agreement with previous experimental data in chimney or detonation soot, suggesting its possible presence in the specimen. *Published by AIP Publishing.* <https://doi.org/10.1063/1.5037380>

I. INTRODUCTION

Carbon is an amazing and versatile element: not only because it is significant and an essential element required for all life processes but also due to its rich physical and chemical properties. Samara Carbon Allotrope Database (SACADA)^{1,2} already indexed more than 500 hypothetical carbon structures, and this number is growing fast. The discovery of fullerenes,³ nanotubes,⁴ and graphene⁵ has motivated tremendous interest in recent years to explore newly carbon structures in sp^3 -, sp^2 -, and sp -hybridized bonding networks. These synthesized carbon allotropes give rise to enormous scientific and technological impacts on natural science, leading to many applications in different fields such as protective coatings, gas sensing, energy storage systems, and solar cells.^{6,7} On the other hand, to guide the experimental synthesis of new carbon allotropes, highly accurate theoretical predictions are indispensable in the search of new carbon forms. To our knowledge, various hypothetical carbon modifications have been proposed theoretically, including the Cco C₈,⁸ bco C₁₆,⁹ bcc C₈,¹⁰ T-carbon,¹¹ T₆-, and T₁₄-carbon.¹² Several predicted allotropes, i.e., monoclinic bct C₄,¹³ and M-carbon¹⁴ were also reported to simulate the synthesized phase. Until recently, there are still other experimental and theoretical efforts made on new carbon materials (i.e., V carbon,¹⁵ 3D-pentagon carbon,¹⁶ and compressed glassy carbon¹⁷). All of the above gives a reason to name the modern time as “the era of carbon allotropes.”¹⁸

In this work, on the basis of the first-principles calculations, we present a theoretical investigation of the structural, mechanical, and electronic properties of the novel carbon allotrope, D-carbon [with the **jbw** topology, the topology naming is based on the reticular chemistry structure resource

(RCSR) database¹⁹ and database of zeolite structures²⁰]. This novel topology structure was also mentioned by Deringer *et al.*²¹ and independently re-discovered in the present work using the structure optimization algorithm. D-carbon can be described as a mixture of **dia** and **sra** nets as we will discuss later. The calculated results demonstrate that D-carbon is dynamically stable and with a lower energy than some previously reported modifications (i.e., C₂₀,²² T₆,¹² and T-carbon¹¹). A satisfactory match of the simulated and measured X-ray diffraction pattern indicates the possible presence of D-carbon in chimney or detonation soot.

II. METHOD AND COMPUTATIONAL DETAILS

The first-principles calculations were based on density functional theory with the generalized gradient approximation (GGA) in the form of the Perdew-Burke-Ernzerhof (PBE) function for the exchange-correlation potential.²³ All calculations were performed using the Vienna *ab initio* Simulation Package (VASP).²⁴ The energy cutoff of the plane wave was set to 650 eV, and the precision of energy convergence was 10^{-5} eV.^{25,26} The atomic positions were fully relaxed until the maximum force on each atom was less than 10^{-3} eV/Å. For a carbon atom, $2s^2 2p^2$ electrons were considered as the valence electrons. The Brillouin zone was sampled with a $10 \times 7 \times 6$ Monkhorst-Pack k-point grid for geometry optimization. Phonon dispersions and density of states (DOS) were performed in the Phonopy package²⁷ interfaced with the density functional perturbation theory (DFPT),²⁸ as performed in VASP. For accurate bandgap estimations, we employed the hybrid functional approach (HSE06).²⁹ The search of stable carbon systems, with six atoms/cell, is also performed using the structure particle swarm optimization (PSO) algorithms, as implemented in the CALYPSO package.^{30,31} First-principles finite temperature molecular dynamics (MD) simulations were performed to further examine the stability of the structure by

^{a)}Electronic mail: lsh@zjut.edu.cn

^{b)}Electronic mail: huxj@zjut.edu.cn

using time steps of 1 fs in $3 \times 3 \times 3$ super-cells containing 162 atoms/cell.

III. RESULTS AND DISCUSSION

We have performed structure prediction using the PSO methodology for carbon containing six atoms in the simulation cell at 0 K. Besides the well-known graphene,⁵ T₆,¹² and T₁₂³² carbon, our simulations also revealed the **jbw** phase which we call D-carbon. Here, we focus our discussion in this work on only this phase (D-carbon), leaving a detailed analysis of all other predicted metastable structures to a follow-up study.

Figure 1 displays the optimized structural model of D-carbon. This structure has an orthorhombic primitive cell containing six C atoms, with a highly symmetric space group $Pm\bar{3}m$ (D_{2h}^5 , 51). Structurally, this novel four-connected net is also familiar in several typical **jbw**-type zeolites.^{33,34} At zero pressure, the relaxed bond lengths of C–C are 1.60 and 1.54 Å, respectively. Figure 2 shows the calculated total energy versus volume and relative enthalpy for D-carbon compared to other previously proposed carbon phases. We note that D-carbon is not only more stable than some theoretically predicted carbon modifications (i.e., T₆ and bcc C₈), but also energetically more favorable than several experimentally realized carbon modifications (i.e., C₂₀ fullerene and T-carbon), implying that the D-carbon could be synthesized. To further evaluate the relative stability of this phase, we also calculated its cohesive energy $E_{coh} = [6E_C - E_{total}]/6$, where E_{total} and E_C are the total energy of D-carbon and a single C atom, respectively. As listed

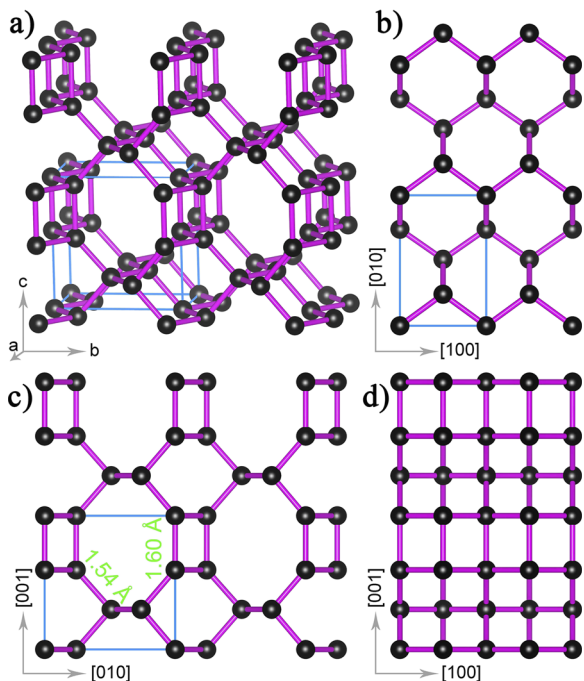


FIG. 1. Crystal structure of D-carbon: (a) perspective view and [(b)–(d)] view along the *c*, *a*, and *b* axis, respectively. At zero pressure, the lattice parameters of D-carbon are $a = 2.52$ Å, $b = 3.91$ Å, and $c = 3.81$ Å, occupying the $2e$ (0.25, 0.00, 0.89) and $4k$ (0.75, 0.71, 0.38) Wyckoff positions, respectively. The unit cell is marked by the blue line, and carbon atoms are plotted with black balls.

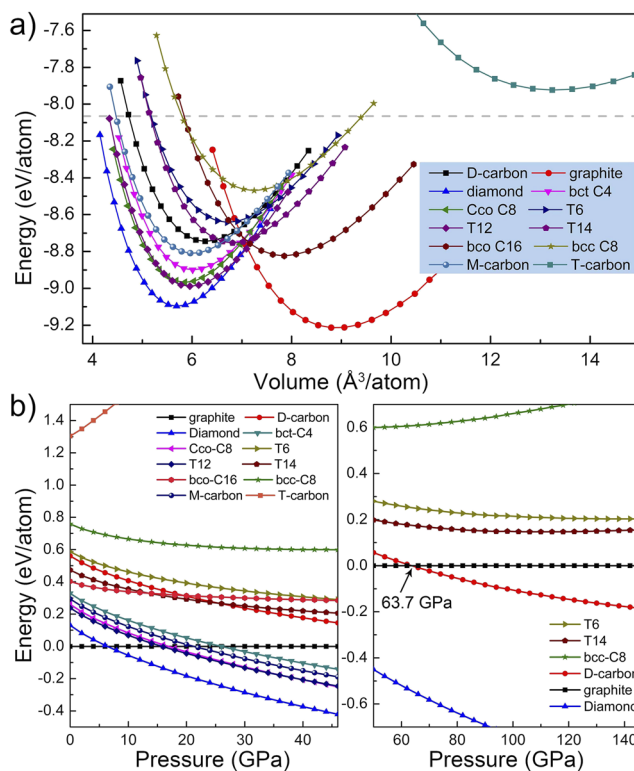


FIG. 2. (a) Calculated energy versus volume per atom for the D-carbon structure compared to graphite, diamond, bct C₄, Cco C₈, T₆, T₁₄, bcc C₁₆, bcc C₈, M-carbon, and T-carbon. The dashed line indicates the energy level of C₂₀ fullerene.²² (b) Calculated relative enthalpies of D-carbon, diamond, bct C₄, Cco C₈, T₆, T₁₄, bcc C₁₆, bcc C₈, M-carbon, and T-carbon with respect to graphite. To highlight the relative stability of D-carbon at high pressure (>50 GPa), we only considered T₆, T₁₄, bcc C₈, diamond, and D-carbon with respect to graphite, as shown in Fig. 2(b), right panel.

in Table S1, the calculated cohesive energy (7.48 eV/atom), apparently higher than previously proposed T-carbon (6.573 eV/atom^{11,35}), suggests that D-carbon is a strongly bonding network. We have also compared the relative energy of D-carbon with others known as carbon allotropes with a 6-atom unit cell (Table S2). As can be seen from Table S2, D-carbon is more stable than many 6-atom structures, including **tft**, **dmd**, and others.

Significantly, with the increase of the pressure, the D-carbon becomes preferable to graphite above 63.7 GPa, which is more stable than earlier theoretical T₆ and T₁₄ structures at this pressure [see Fig. 2(b)]. Furthermore, the phonon spectrum and phonon DOS indicate that D-carbon is dynamically stable, both at zero pressure and high pressure (see Fig. S1). Therefore, once synthesized, D-carbon should be quenchable as a metastable phase to ambient pressure and low temperatures. The highest phonon frequency is located at the Γ point with a value of ≈ 1333 cm⁻¹, which is lower than graphite (≈ 1600 cm⁻¹), but close to graphite at 63.7 GPa. The thermal stability of D-carbon was also confirmed by analyzing the backbone root-mean-square deviation (RMSD) from the starting crystal configuration over the process of the trajectory. It is evident that the RMSD levels off to ≈ 3.7 Å at 1000 K, indicating that the geometric configuration is expected to be remarkably stable (see Fig. S1).

D-carbon has nine independent elastic constants C_{ij} ; for a stable orthorhombic structure, its corresponding elastic constants C_{ij} should satisfy the following elastic stability criteria: $C_{11}, C_{22}, C_{33}, C_{44}, C_{55},$ and $C_{66} > 0$, $[C_{11} + C_{22} + C_{33} + 2(C_{12} + C_{13} + C_{23})] > 0$, $[C_{11} + C_{22} - 2C_{12}] > 0$, $[C_{11} + C_{33} - 2C_{13}] > 0$, and $[C_{22} + C_{33} - 2C_{23}] > 0$ for the orthorhombic phase.⁹ The calculated elastic constants $C_{11}, C_{22}, C_{33}, C_{44}, C_{55}, C_{66}, C_{12}, C_{13},$ and C_{23} are 1036, 737, 867, 290, 371, 415, 48, 59, and 236 GPa, respectively. Distinctly, the calculated elastic constants meet this criterion, indicating that it is mechanically stable. The density of D-carbon is 3.20 g/cm^3 , which is comparable to that of bct C_4 (3.32 g/cm^3), but drastically higher than T-carbon (1.50 g/cm^3) (see Table S1). Vickers hardness (H_V) of D-carbon is 86.58 GPa, which is calculated by the empirical formula $H_V \text{ (GPa)} = 350[(Ne^{2/3})e^{-1.191/f_i}]/d^{2.5}$,³⁶ where Ne is the electron density of the number of valence electrons per cubic angstroms, d is the bond length, and f_i is the ionicity of the chemical bond in a crystal scaled by Phillips.³⁷ The calculated Vickers hardness of diamond in this work is 92.49 GPa, closing to the previously theoretical (93.6 GPa) and experimental value ($96 \pm 5 \text{ GPa}$) (see Table S1). However, this model and similar models³⁸ have been shown to overestimate the hardness of materials such as T-carbon,³⁹ especially when the material is anisotropic. Therefore, to consider the anisotropy of D-carbon (*vide infra*), we also use different hardness models based on the elastic moduli, i.e., Teter,⁴⁰ Chen *et al.*,⁴¹ and Tian *et al.*⁴² All of these methods have been applied to many carbon allotropes successfully. The calculated hardness values of D-carbon are 54.4 GPa, 57.8 GPa, and 57.7 GPa, using the Teter, Chen *et al.*, and Tian *et al.* methods, respectively. For comparison, the hardness values of diamond are 80.6 GPa, 95.3 GPa, and 97.3 GPa using

the same models. Therefore, the elastic moduli based hardness methods demonstrate that D-carbon is significantly softer than diamond. According to the generally accepted convention, superhard materials are considered to have a H_V exceeding 40 GPa;⁴³ therefore, D-carbon can be regarded as a superhard material.

Stress-strain curves for D-carbon under various strains are shown in Fig. 3(a). The ideal strength of D-carbon is strongly anisotropic. Interestingly, tensile stress-strain curves along [010], [100], and [011] show a plastic deformation relation, which is consistent with the ductility of D-carbon compared with diamond. D-carbon with [101] orientation presents the largest ideal strength of 133 GPa, and critical strain reaches to 0.21. However, with the [011] direction, D-carbon shows the smallest ideal strength and critical strain (73 GPa and 0.16), giving rise to the (001) easy cleavage planes. In the (101) lattice plane, its pure shear stress along the [100] direction has the highest peak value (122 GPa), which is moderately lower than the (111)- $[\bar{1}\bar{1}2]$ direction of diamond (140 GPa),⁴⁴ but still obviously higher than the (100)- $\langle 001 \rangle$ slip orientation of T-carbon (7.3 GPa),³⁹ while the $[0\bar{1}0]$ direction has the lowest peak value (82 GPa). Under indentation shear deformation, the stress response is almost identical to that under pure shear deformation, but pure shear strain causes greatly enhanced stiffness.

Figure 4(a) shows the orbitally resolved band structure of D-carbon. It is insulating with an indirect bandgap. The PBE bandgap is 3.15 eV. The HSE correction does not change the band structure qualitatively, but increases the bandgap to 4.33 eV (see Fig. S2), which is smaller than diamond. The results demonstrate that the valence band maximum (VBM) of D-carbon is contributed by C_{2px} states, while the conduction

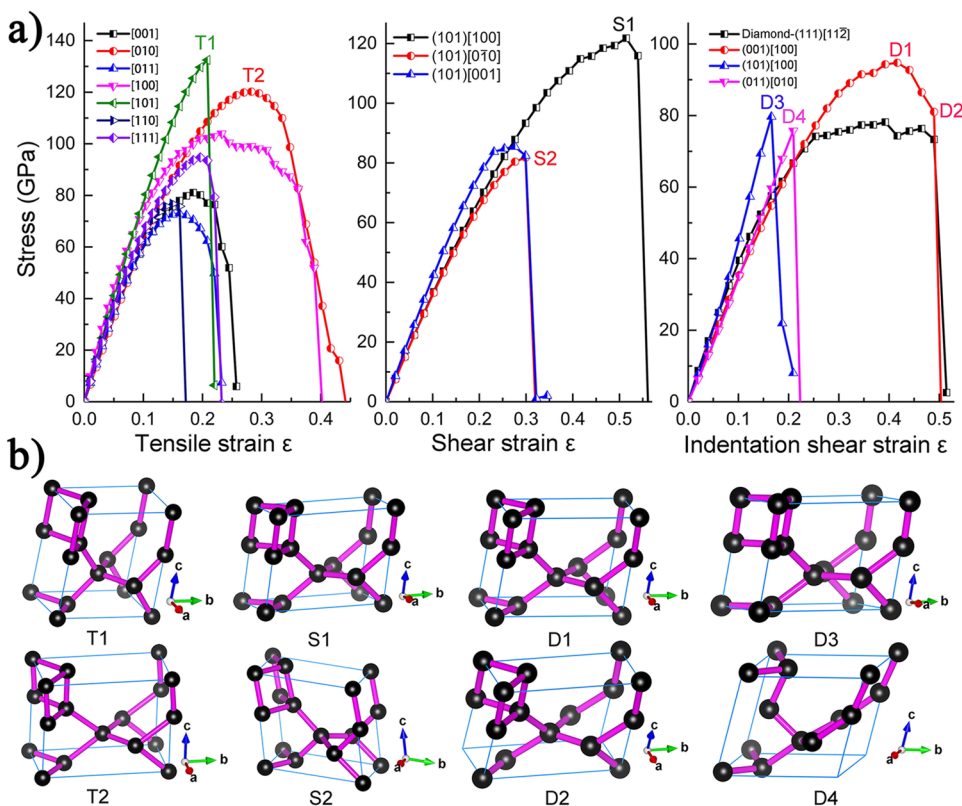


FIG. 3. (a) Calculated stress responses under pure tensile (left), pure shear (center), and indentation shear (right) strains along various high-symmetry directions, respectively. (b) The structural snapshots at different key points after the large deformation of stress on each stress-strain curve under pure tensile, pure shear, or indentation shear strains.

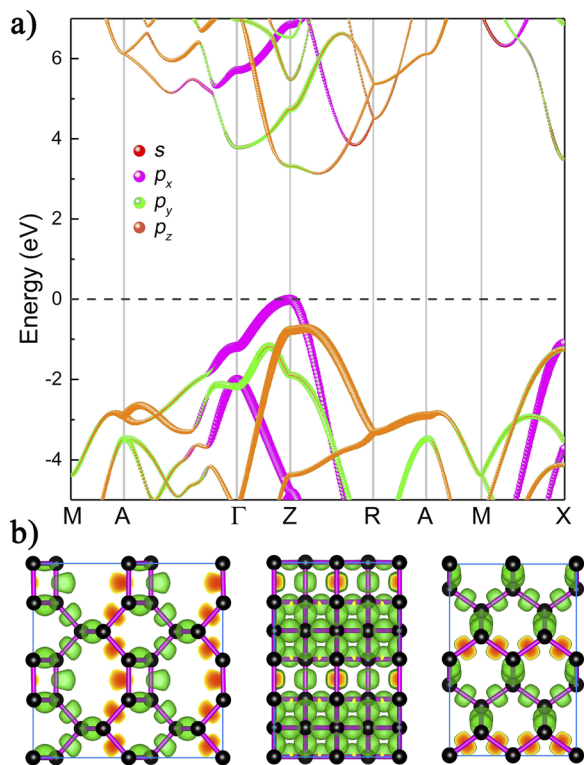


FIG. 4. (a) Electronic band structure of D-carbon decomposed with respect to the C_s , C_{p_x} , C_{p_y} , and C_{p_z} orbitals calculated by the PBE functional. (b) Calculated ELF of D-carbon at 0 GPa. The isosurface value is set as 0.75.

band minimum (CBM) is mainly contributed by C_{2p_z} states. There is an obvious orbital hybridization between C_{2s} and C_{2p} states below the Fermi level. To investigate the bonding state between the C–C atoms, we calculated its electron localization function (ELF). From Fig. 4(b), the D-carbon is an all- sp^3 carbon modification with all electrons well localized between the C–C atoms forming the σ bonds.

To further establish the experimental connection of our proposed structure, we have simulated the X-ray diffraction (XRD) patterns to compare with the experimental data (Fig. 5). Different from diamond where the peaks of (111) at 44° are observed, for D-carbon, the peaks at 22.7° , 23.3° , 32.8° , and 43.1° are clearly visible. For chimney or detonation soot, the most distinct feature of the experimental measured XRD spectra is the peak around 23° that does not match any previously known carbon phases.^{45,46} Our simulated XRD results show that the diffraction peaks of D-carbon satisfactorily match the previously unexplained peak, even though the peaks are broad. Within a reasonable range of the error between theoretical calculation and experimental measurement (i.e., the presence of stress), it must be pointed out that our calculated data still match well with the experimental results in the chimney or detonation soot (i.e., the peaks around 23° , 43.5° , 66° , and 83°) compared with previous work.⁴⁷ These results suggest that D-carbon is a possible candidate of the carbon phase observed in the chimney or detonation soot.

The simulated Raman and Infrared (IR) vibrational modes with corresponding frequencies are presented in Fig. S3. The Raman and IR spectra exhibit distinguishing lines at 1075 cm^{-1} and 1239 cm^{-1} , respectively. These attainable

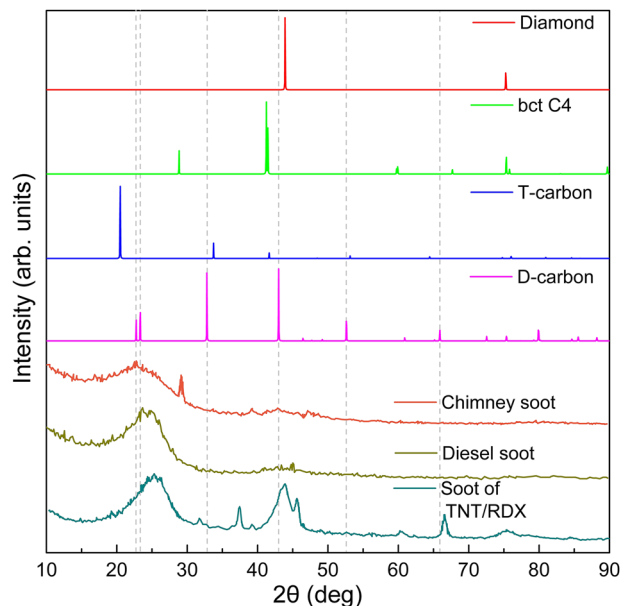


FIG. 5. The simulated XRD patterns of diamond, bct C_4 , T-carbon, and D-carbon are compared with experimental data. The experimental XRD patterns are from Refs. 45 and 46. The used X-ray wavelength is 1.54 \AA , as employed in the experiment.⁴⁶

features may be helpful for identifying the D-carbon experimentally. We also suggest a plausible reaction route for the D-carbon structure by using polyethylene chains via dehydrogenation and assembly, as shown in Fig. S4. Although the real experimental environment is extremely complex, but to some degree, we can still provide some theoretical guidance to the experimental synthesis.^{16,48} Given the energetic favorability and high dynamic stability of D-carbon and in consideration of the rapid development in experimental techniques which have synthesized some novel carbon allotropes recently,^{15,49} we expect that D-carbon could be fabricated experimentally.

Next, we decomposed D-carbon with the **jbw** topology into building units to find the relation between the D-carbon and other three-periodic carbon allotropes from the SACADA database. Decomposition was carried out by means of the algorithm of searching for the natural tiling⁵⁰ that is implemented in the ToposPro⁵¹ program package. The 3dt⁵² program was used for the visualisation of the building units and way of its assembling. As has been previously shown, the tiling approach can be useful to predict as well as classify and compare allotropes.⁵³

The **jbw** net is constructed from two types of building units in a one-to-one ratio, adamantane cage 4^6 (which formed by a four six-member ring) of diamond [Fig. 6(a)], and $4^2.6^2.8^2$ cage [Fig. 6(e)] of the **sra** net. The $4^2.6^2.8^2$ cage can be considered as the extended 4^6 adamantane cage. Due to the close geometry and topology of the building units, diamond and **sra** nets have the same way of self-assembling (Fig. 6). The building blocks are connecting to each other through common 6- [Fig. 6(b)] and 8-membered rings [Fig. 6(f)], respectively, forming one-periodic chains. The chains are joined in two-periodic layers by means of a common zigzag-like simply connected [Fig. 6(c)] and ladder [Fig. 6(g)] chain. Finally, the nets are assembling from

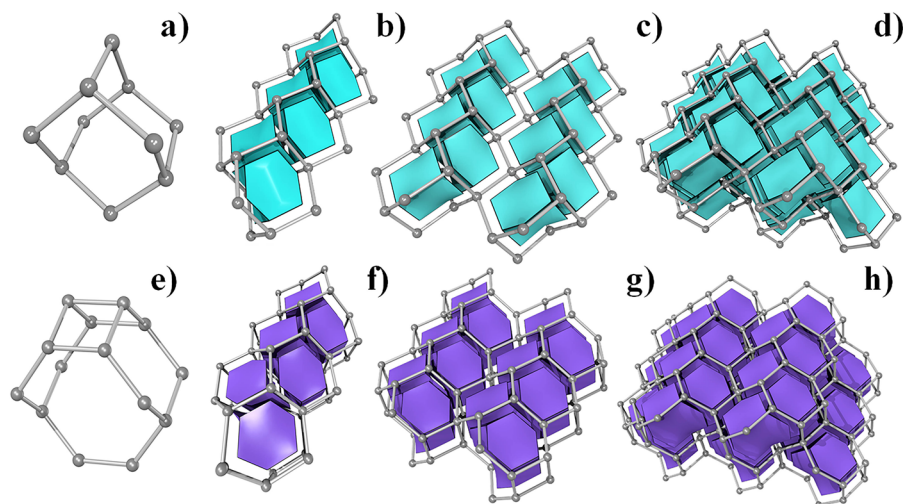


FIG. 6. The building schemes of diamond [(a)–(d)] and **sra** [(e)–(h)] nets.

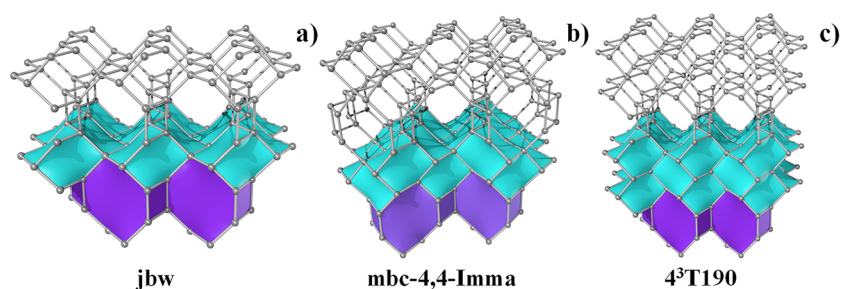


FIG. 7. The assembling schemes of **jbw** (a), **mbc-4,4-Imma** (b), and 4^3T190 (c) nets from diamond (aquamarine) and **sra** (violet) layers.

the layers through common 6-membered rings [Figs. 6(d) and 6(h)].

In both cases, the external surface of the **dia** and **sra** layers is a distorted graphene-like surface. Consequently, the layers are complementary and can be used to construct new nets. Theoretically an infinite number of topologically inequivalent nets can be obtained by means of various combinations of the layers. However, only a few of such nets (Fig. 7) were reported as possible carbon allotropes: **jbw**, **mbc-4,4-Imma**, and 4^3T190 .

All these allotropes are hybrids of diamond and carbon structures with the **sra** topology, which was first reported as 8-tetra(3,3) tubulane. In this way, the allotropes should have intermediate properties between diamond and 8-tetra(3,3)tubulane (Table S3). The structure of the diamond has the lowest energy and the higher density in comparison with the structure of the 8-tetra(3,3)tubulane. As a result, the increase of the amount of diamond layers in the structures decreases energy and increases the density (Table S3) of the allotropes.

IV. CONCLUSIONS

In summary, the D-carbon, an orthorhombic sp^3 bonded structure with the **jbw** topology, was studied theoretically using the first-principles calculations. This structure is energetically more stable than several previously proposed sp^3 carbon allotropes with 6 atoms/cell. The results in this work indicate that D-carbon is another potential modification of the metastable sp^3 carbon system. These results provide deep

insight into the physical properties of D-carbon with an unusual structural motif and high dynamic stability, but also promote further investigations on the novel carbon allotropes with desirable electronic and mechanical properties.

SUPPLEMENTARY MATERIAL

See [supplementary material](#) for the details of structural parameter, phonon dispersion curves, MD result, HSE06 band structure, Raman, and IR spectra of the D-carbon.

ACKNOWLEDGMENTS

This work was supported by the National Natural Science Foundation of China (Grant Nos. 11504325, 50972129, and 50602039) and Natural Science Foundation of Zhejiang Province (Grant No. LQ15A040004). This work was also supported by the international science technology cooperation program of China (Grant No. 2014DFR51160), the National Key Research and Development Program of China (Grant No. 2016YFE0133200), and the One Belt and One Road International Cooperation Project from the Key Research and Development Program of Zhejiang Province (Grant No. 2018C04021). A.A.K. thanks the Russian Foundation for Basic Research for partial support with Grant No. 16-32-00296 mol.a and the Russian Ministry of Science and Education for partial support with Grant No. 3.7626.2017/9.10. The authors gratefully acknowledge the suggestions and advice of Professor D. M. Proserpio.

There are no conflicts to declare.

- ¹R. Hoffmann, A. A. Kabanov, A. A. Golov, and D. M. Proserpio, *Angew. Chem., Int. Ed.* **55**, 10962 (2016).
- ²D. M. Proserpio, A. A. Kabanov, and A. A. Golov, Carbon allotropes database, see <http://sacada.sctms.ru>, 2016.
- ³W. Krätschmer, L. D. Lamb, K. Fostiropoulos, and D. R. Huffman, *Nature* **347**, 354 (1990).
- ⁴S. Iijima and T. Ichihashi, *Nature* **363**, 603 (1993).
- ⁵K. S. Novoselov, A. K. Geim, S. V. Morozov, D. Jiang, Y. Zhang, S. V. Dubonos, I. V. Grigorieva, and A. A. Firsov, *Science* **306**, 666 (2004).
- ⁶J. Lee, J. Kim, and T. Hyeon, *Adv. Mater.* **18**, 2073 (2006).
- ⁷A. A. Balandin, *Nat. Mater.* **10**, 569 (2011).
- ⁸Z. Zhao, B. Xu, X.-F. Zhou, L.-M. Wang, B. Wen, J. He, Z. Liu, H.-T. Wang, and Y. Tian, *Phys. Rev. Lett.* **107**, 215502 (2011).
- ⁹J.-T. Wang, H. Weng, S. Nie, Z. Fang, Y. Kawazoe, and C. Chen, *Phys. Rev. Lett.* **116**, 195501 (2016).
- ¹⁰R. L. Johnston and R. Hoffmann, *J. Am. Chem. Soc.* **111**, 810 (1989).
- ¹¹X.-L. Sheng, Q.-B. Yan, F. Ye, Q.-R. Zheng, and G. Su, *Phys. Rev. Lett.* **106**, 155703 (2011).
- ¹²S. Zhang, Q. Wang, X. Chen, and P. Jena, *Proc. Natl. Acad. Sci. U. S. A.* **110**, 18809 (2013).
- ¹³K. Umemoto, R. M. Wentzcovitch, S. Saito, and T. Miyake, *Phys. Rev. Lett.* **104**, 125504 (2010).
- ¹⁴Q. Li, Y. Ma, A. R. Oganov, H. Wang, H. Wang, Y. Xu, T. Cui, H.-K. Mao, and G. Zou, *Phys. Rev. Lett.* **102**, 175506 (2009).
- ¹⁵X. Yang, M. Yao, X. Wu, S. Liu, S. Chen, K. Yang, R. Liu, T. Cui, B. Sundqvist, and B. Liu, *Phys. Rev. Lett.* **118**, 245701 (2017).
- ¹⁶C. Zhong, Y. Chen, Z.-M. Yu, Y. Xie, H. Wang, S. A. Yang, and S. Zhang, *Nat. Commun.* **8**, 15641 (2017).
- ¹⁷M. Hu, J. He, Z. Zhao, T. A. Strobel, W. Hu, D. Yu, H. Sun, L. Liu, Z. Li, M. Ma *et al.*, *Sci. Adv.* **3**, e1603213 (2017).
- ¹⁸A. Hirsch, *Nat. Mater.* **9**, 868 (2010).
- ¹⁹M. O’Keeffe, M. A. Peskov, S. J. Ramsden, and O. M. Yaghi, *Acc. Chem. Res.* **41**, 1782 (2008).
- ²⁰C. Baerlocher, Database of Zeolite Structures, see <http://www.iza-structure.org/databases/>, 2008.
- ²¹V. L. Deringer, G. Csányi, and D. M. Proserpio, *ChemPhysChem* **18**, 873 (2017).
- ²²H. Prinzbach, A. Weiler, P. Landenberger, F. Wahl, J. Wörth, L. T. Scott, M. Gelmont, D. Olevano, and B. von Issendorff, *Nature* **407**, 60 (2000).
- ²³J. P. Perdew, K. Burke, and M. Ernzerhof, *Phys. Rev. Lett.* **77**, 3865 (1996).
- ²⁴G. Kresse and J. Furthmüller, *Phys. Rev. B* **54**, 11169 (1996).
- ²⁵D. Fan, S. Lu, Y. Guo, and X. Hu, *J. Mater. Chem. C* **5**, 3561 (2017).
- ²⁶D. Fan, S. Lu, Y. Guo, and X. Hu, *J. Mater. Chem. C* **6**, 1651 (2018).
- ²⁷A. Togo and I. Tanaka, *Scr. Mater.* **108**, 1 (2015).
- ²⁸S. Baroni, S. De Gironcoli, A. Dal Corso, and P. Giannozzi, *Rev. Mod. Phys.* **73**, 515 (2001).
- ²⁹J. Heyd, G. E. Scuseria, and M. Ernzerhof, *J. Chem. Phys.* **118**, 8207 (2003).
- ³⁰Y. Wang, J. Lv, L. Zhu, and Y. Ma, *Phys. Rev. B* **82**, 094116 (2010).
- ³¹Y. Wang, J. Lv, L. Zhu, and Y. Ma, *Comput. Phys. Commun.* **183**, 2063 (2012).
- ³²Z. Zhao, F. Tian, X. Dong, Q. Li, Q. Wang, H. Wang, X. Zhong, B. Xu, D. Yu, J. He *et al.*, *J. Am. Chem. Soc.* **134**, 12362 (2012).
- ³³A. Healey, P. Henry, G. Johnson, M. Weller, M. Webster, and A. Genge, *Microporous Mesoporous Mater.* **37**, 165 (2000).
- ³⁴A. Tripathi and J. B. Parise, *Microporous Mesoporous Mater.* **52**, 65 (2002).
- ³⁵J. Zhang, R. Wang, X. Zhu, A. Pan, C. Han, X. Li, D. Zhao, C. Ma, W. Wang, H. Su *et al.*, *Nat. Commun.* **8**, 683 (2017).
- ³⁶F. Gao, J. He, E. Wu, S. Liu, D. Yu, D. Li, S. Zhang, and Y. Tian, *Phys. Rev. Lett.* **91**, 015502 (2003).
- ³⁷J. Phillips, *Rev. Mod. Phys.* **42**, 317 (1970).
- ³⁸A. Šimnek and J. Vackář, *Phys. Rev. Lett.* **96**, 085501 (2006).
- ³⁹X.-Q. Chen, H. Niu, C. Franchini, D. Li, and Y. Li, *Phys. Rev. B* **84**, 121405 (2011).
- ⁴⁰D. M. Teter, *MRS Bull.* **23**, 22 (1998).
- ⁴¹X.-Q. Chen, H. Niu, D. Li, and Y. Li, *Intermetallics* **19**, 1275 (2011).
- ⁴²Y. Tian, B. Xu, and Z. Zhao, *Int. J. Refract. Met. Hard Mater.* **33**, 93 (2012).
- ⁴³V. L. Solozhenko, D. Andrault, G. Fiquet, M. Mezouar, and D. C. Rubie, *Appl. Phys. Lett.* **78**, 1385 (2001).
- ⁴⁴Y. Zhang, H. Sun, and C. Chen, *Phys. Rev. B* **73**, 144115 (2006).
- ⁴⁵P. Chen, F. Huang, and S. Yun, *Carbon* **41**, 2093 (2003).
- ⁴⁶D. Pantea, S. Brochu, S. Thiboutot, G. Ampleman, and G. Scholz, *Chemosphere* **65**, 821 (2006).
- ⁴⁷Y. Liu, X. Jiang, J. Fu, and J. Zhao, *Carbon* **126**, 601 (2018).
- ⁴⁸X. Jiang, J. Zhao, Y.-L. Li, and R. Ahuja, *Adv. Funct. Mater.* **23**, 5846 (2013).
- ⁴⁹P. Liu, H. Cui, and G. Yang, *Cryst. Growth Des.* **8**, 581 (2008).
- ⁵⁰V. A. Blatov, O. Delgado-Friedrichs, M. O’Keeffe, and D. M. Proserpio, *Acta Crystallogr., Sect. A: Found. Crystallogr.* **63**, 418 (2007).
- ⁵¹V. A. Blatov, A. P. Shevchenko, and D. M. Proserpio, *Cryst. Growth Des.* **14**, 3576 (2014).
- ⁵²C. Baerlocher, Generation, Analysis and Visualization of Reticular Ornaments, see <http://gavrog.org/>, 2017.
- ⁵³I. A. Baburin, D. M. Proserpio, V. A. Saleev, and A. V. Shipilova, *Phys. Chem. Chem. Phys.* **17**, 1332 (2015).